



ELSEVIER

International Journal of Mass Spectrometry 181 (1998) 159–165



# Spectrum recovery from discrete detector arrays— correction for nonuniformity

K. Birkinshaw\*

*Department of Physics, University of Wales Aberystwyth, Aberystwyth, Ceredigion SY23 3BZ, UK*

Received 21 July 1998; accepted 13 September 1998

## Abstract

In arrays of detectors there is always a degree of nonuniformity. The causes of nonuniformity are outlined for the case of an array of independent detectors and an algorithm is presented that enables nonuniformity correction and recovery of the spectrum incident on the detector from the measured spectrum under the conditions given. (Int J Mass Spectrom 181 (1998) 159–165) © 1998 Elsevier Science B.V.

*Keywords:* Detector; Array; Uniformity; Performance

## 1. Introduction

An array of detectors with all associated electronics has been integrated on a single silicon chip at Aberystwyth for use in mass spectrometry (Langstaff et al. [1]). Whereas many problems have been resolved, there remains a problem that affects all arrays, namely nonuniformity due to manufacturing tolerances.

A spatially dispersed spectrum can be conveniently measured using a single-slit detector. The slit defines the segment of spectrum being measured and hence the resolving power. The question of uniformity does not arise for a single detector. Arrays of detectors allow the detection of particles at many positions in the focal plane of a spectrometer and enable a large increase in efficiency, but nonuniformity to a greater

or lesser extent is always present. There are a variety of types of arrays available that have been reviewed previously (Richter and Ho [2], Smith [3], Birkinshaw [4]). This article investigates the problem of nonuniformity in discrete detector arrays. Fig. 1 (a) shows a schematic of a single-slit detector in a mass spectrometer.

By replacing the single-slit detector with an array of detectors, a much larger fraction of the spectrum can be measured. The example of Fig. 1 (b) shows a “discrete detector” array, i.e. an array of discrete or independent detectors. A particle falling on the microchannel plate electron multiplier (MCP) initiates a pulse of electrons from a small area of the MCP exit that falls on the detector electrodes (detector inputs) and is detected. The MCP enables amplification of the incoming particle flux while retaining the spatial information. Generally, a single MCP pulse is registered as a single count on a group of  $N$  detectors where  $N$  depends on the pulse gain, MCP/array

\* Corresponding author.

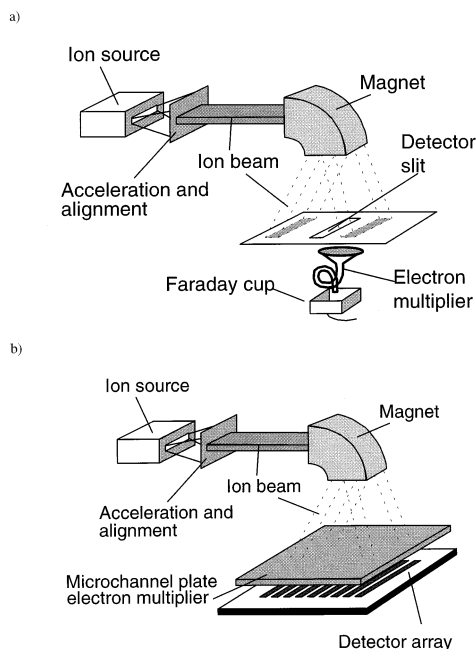


Fig. 1. Simplified schematic of a magnetic sector mass spectrometer incorporating (a) a single-slit detector, and (b) a discrete detector array in which the slit of the single detector is replaced by a one dimensional array of metal strips (electrodes) each of which has approximately the same dimensions as the single slit. Each electrode collects charge from the MCP output and forms the input to a detector circuit.

separation, etc. and has been observed to vary from 0 [observable only indirectly (Narayan et al. [5]) to 14. Much smaller values of  $N$  are seen (e.g.  $N = 1-3$ ) if the MCP/array separation is small (e.g.  $4.5 \mu\text{m}$ ). Sources of nonuniformity are summarized in Table 1. It is clear that even for a “perfect” detector array

Table 1  
Sources of nonuniformity

MCP	Array <sup>a</sup>
Channel to channel variations; Longer range variations; Separation between MCP output and array surface; Waviness; Accuracy of mounting	Sampling frequency limited by spatial resolution of detectors; Sensitivity variation (variation in circuitry sensitivity and variation in capacitance of electrode)

<sup>a</sup> Note that the relative positions of detector electrodes on the silicon chip are known extremely accurately—typically to  $1 \mu\text{m}$  in 1 cm.

nonuniformity could be attributed to the MCP and the mounting accuracy.

### 1.1. Measured spectra

A measured spectrum is an accumulation of many single events. Nonuniformities may or may not be canceled out during accumulation of these events. For example, many MCP channels may service a single detector site and it would be expected that short range (channel to channel) variation of MCP performance would cancel out. On the other hand variation of detector sensitivity would not.

A single event may be visualized as the following sequence of events (Fig. 2). An ion enters an MCP channel in the first of two MCP plates and initiates an electron pulse of typically  $10^4$  electrons from the channel, i.e. the gain is typically  $10^4$ . These electrons enter a number of channels of the second plate. Because these channels are activated by a large number of electrons each channel is driven to saturation and outputs typically  $10^6$  electrons. At saturation the gain is independent of the initiating event and the distribution of gains for many events is peaked. As shown in Fig. 2 (a) and (b) an MCP output pulse typically covers several detector electrodes and a voltage is induced on each electrode whose magnitude depends on the amount of electron charge.

There is necessarily no slit to define the incident ion beam on the MCP or the output pulse charge falling on the detectors. A given detector is affected by all the MCP output pulses; the more remote the pulse, the smaller the voltage induced on a given detector. The function of a defining slit is performed by the pulse height discrimination level (PHDL) of the detectors. These are ideally the same across the array. An externally supplied voltage varies the PHDLs in unison. A schematic of voltage distributions induced on detector electrodes due to a single MCP pulse is shown in Fig. 2 (b). With the PHDL shown a single count is recorded on three detectors. The value of  $N$  would be higher for a lower PHDL and lower for a higher PHDL. Fig. 2 (c) shows a number of single events measured by the array with the count group size  $N$  varying from 1–3. For many

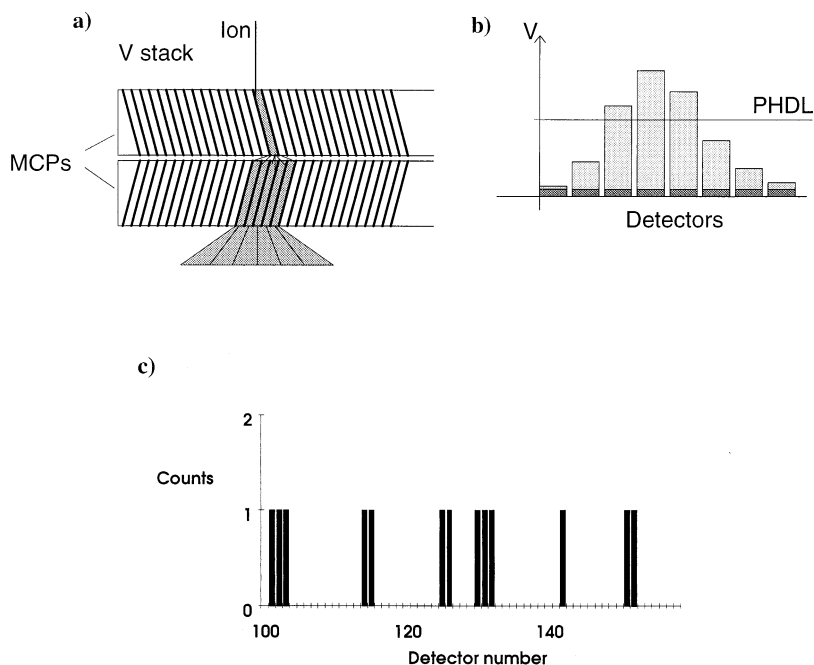


Fig. 2. (a) A single event leads to a wide electron pulse at the MCP exit with further spreading on traveling to the array. The MCP channels are arranged to slope in opposite directions to reduce ion feedback and optimize the incident ion detection efficiency. (b) Voltage pulses induced on detector electrodes by a single event. A wide electron pulse falls on several electrodes giving voltage pulses  $>$  PHDL on  $N$  ( $= 3$  in this case) electrodes. (c) Single events measured by the array. It has been observed that count groups of up to 14 detectors can be activated by a single ion for a large MCP/array separation. At low separation (e.g.  $4.5 \mu\text{m}$ )  $N = 1-3$ .

events there will be a distribution of pulse voltages on a given detector electrode. These are represented in Fig. 3 where it is assumed that all the incident ions are centered at detector  $m$ . Further away from the peak centre the pulse height distributions are peaked at lower voltages and a smaller fraction of pulses are detected. No pulses are detected on detector  $m-3$  because the pulse height distribution lies completely below the PHDL. Nonuniformity can now be characterized as a result of (1) nonuniform PHDLs across the array resulting in incorrect fractions of the pulse height distributions being measured, and (2) distortion of MCP pulse height distributions due to nonuniform MCP performance. The pulse height distribution on a single detector due to an incident spectrum covering many detectors is attributed to all events giving a much broader distribution than that due to a single narrow peak. Therefore the error in the measured signal on a given detector whose PHDL is shifted because of nonuniformity depends on the *incident*

*spectrum* and a constant multiplicative correction factor cannot be used. For example, in the case shown in Fig. 3 the detector  $m$  lying at the position of the incident peak measures all ions because the pulse height distribution lies completely above the PHDL of the detector. A small shift of the PHDL (due to nonuniformity) would not affect the measured signal. However, the measured signal on detector  $m-2$  would be measured incorrectly if the PHDL were shifted. Therefore the problem is to correct a measured spectrum when the correction required depends on the incident spectrum as well as the nonuniformity of the detector performance and the MCP performance. Nonuniformity in one dimension (the dimension parallel to the direction of dispersion) is considered in detail here. Nonuniformity in a second spatial dimension is considered at the end of Sec. 2. The second dimension could be ion intensity in which case nonlinear response at higher local ion intensities could be corrected until the limit of complete saturation.

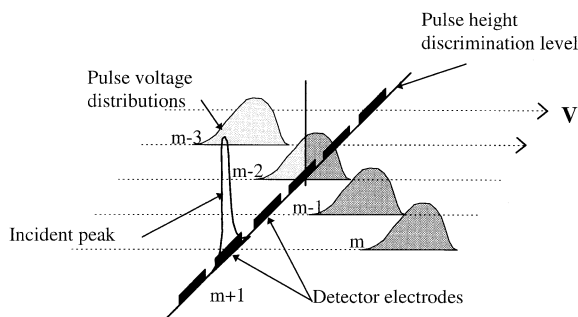


Fig. 3. Assuming a narrow incident beam falling on detector electrode  $m$ , the pulse height distribution will be greatest at detector  $m$  and will shift to lower voltages with increasing distance from the incident beam. Pulse voltages lying above the discrimination level (dark shading) will be recorded and others (light shading) will be rejected. In this figure the PHDLs (diagonal line) of all detectors are the same. Nonuniform PHDLs would result in an incorrect fraction of a pulse distribution being measured.

## 2. Nonuniformity correction

### 2.1. Detector response curves

Consider a narrow incident ion beam moved away from a given detector. When the beam is directly above the detector the induced voltage pulse height distribution on the detector lies at its maximum position and (in the present example of Fig. 3) all ions are detected. When the ion beam is further away from the detector a smaller fraction of the ions is detected. The curve representing the fraction of events measured by a detector as a function of distance of the beam from the detector will be called the detector response curve or DRC. The following are three possible ways of measuring DRCs.

#### 2.1.1. Direct measurement

By stepping a narrow ion beam of fixed intensity across an array to lie sequentially above each detector the response curve of a particular detector can be found by noting the number of events measured as a function of distance of the beam from the detector. Alternatively, the measured ion peak profile can be used in the correction algorithm as explained in Sec. 2.2. The ion beam should be of the same width as a

detector electrode and have a rectangular intensity profile.

#### 2.1.2. Single event analysis

In the analysis of single events (Sinha et al. [6]) the location of each event is given approximately by the centre of mass of the pulse group with an accuracy of about half a detector. By uniformly illuminating the array, ions arrive randomly at all locations and hence detector response curves can be found. For example, after many single events have been observed, then for each detector the fraction of events detected as a function of distance from the detector can be found. Alternatively, all events whose centres are at a given location can be summed to give the peak that would be measured for an incident peak at that location and this can be used in the correction algorithm as explained in Sec. 2.2. It should be noted that there is an element of uncertainty in the location of the event centres because of the nonuniformity itself, and although this uncertainty is believed to be only about half an electrode this method of finding the DRCs requires further evaluation. Measurement of the DRCs could be under software control and fully automated.

#### 2.1.3. Simulation

The nonuniformity of the pulse height discrimination levels of the array can be measured on the bench (Birkinshaw and Langstaff [7]). Using a simulator developed previously (Narayan et al. [8]) the experiments suggested in Secs. 2.1.1 and 2.1.2 can be simulated. This does not correct for nonuniformity of the MCP and mounting but may enable good estimates of the correction matrix  $a^{-1}$  (below) to be found from bench tests.

It is assumed below that (1) the incident spectrum can be approximated by a histogram, and (2) the detector response curves are found as in Sec. 2.1.1 by placing a square profile incident beam above each detector in turn. These are the basic assumptions made in the present work. Further work is progressing to remove these restrictions. Note that where particles fall directly on detector sites (e.g. photons on a CCD) without the intervention of any amplifying or distort-

ing element (e.g. MCP, glass window) and without coupling between detectors, then a straightforward linear correction for nonuniformity can be made. For example, the photosites of a CCD may be nonuniform in (1) their generation of thermal electrons, and (2) their quantum efficiency, but the former can be corrected by addition of a constant factor (at a given temperature and measurement period) and the latter by multiplying the photon intensity by a constant factor.

## 2.2. Nonuniformity correction

With a matrix ( $A$ ) whose rows are the detector response curves, the spectrum incident on the MCP can be represented as a column vector ( $B$ ) and the spectrum measured ( $C$ ) is simply the product of  $A$  and  $B$ :

$$C = A \cdot B$$

Fig. 4 (a) shows a  $10 \times 10$  part of the  $20 \times 20$  matrix  $A$  used to generate Fig. 4 (b) and (c). For example, the fifth (say) element of the vector  $C$  (the observed signal on the fifth detector) is given by multiplying the fifth row of  $A$  (the DRC for the fifth detector) by the incident spectrum  $B$ .

Each detector response curve can in principle be any curve, and for the purposes of demonstrating the algorithm it is justifiable to select any matrix  $A$ . The matrix  $A$  shown below represents a possible nonuniform detector array and the incident spectrum is given in  $B$ . The measured spectrum is shown as the histogram in Fig. 4 (b). Ideally, for a uniform array, all detector response curves should be equal. Matrix  $S$  is an example of an ideal matrix in which each DRC is the same and it therefore represents a uniform array. The “symmetrized” DRCs in  $S$  are chosen to be close to the nonsymmetric DRCs in  $A$  although mathematically this is not necessary. We can write:

$$A = a \cdot S$$

$$\therefore A \cdot S^{-1} = a \cdot S \cdot S^{-1} = a$$

enabling calculation of  $a$  for any  $S$ . Therefore we can write:

$$C = a \cdot S \cdot B$$

$$\therefore a^{-1} \cdot C = a^{-1} \cdot a \cdot S \cdot B = S \cdot B = C_{\text{corr}}$$

and  $C_{\text{corr}}$  is the corrected spectrum that would be seen with a uniform array represented by  $S$ . Therefore  $a^{-1}$  is the correction matrix we require. It should be noted that mathematically the matrix  $S$  could equally well have been any other symmetric matrix including the unit matrix. In the latter case:

$$A = a \cdot I$$

$$\therefore a = A$$

and the correction matrix is  $A^{-1}$ . This of course corresponds to the direct recovery of the incident spectrum from the measured spectrum and follows immediately from  $A \cdot B = C$  since:

$$A^{-1} \cdot A \cdot B = A^{-1} \cdot C = B_{\text{rec}}$$

where  $B_{\text{rec}}$  is the recovered incident spectrum. Calculations show  $C_{\text{corr}}$  to be less sensitive than  $B_{\text{rec}}$  to random fluctuations of  $A$  and  $C$  and gives a more reliable correction.

Fig. 4 (b) shows the measured spectrum  $C$  (histogram) and the spectrum corrected for nonuniformity  $C_{\text{corr}}$  (circles). Fig. 4 (c) shows the incident spectrum (histogram) and the recovered spectrum (circles) that matches the incident spectrum. These results are summarized in Table 2. The input spectrum is peak1 (P1) and peak2 (P2) of vector  $B$ . Vector  $C$  shows the measured peaks and it can be seen that both the peak centroids and the relative total counts are shifted. However,  $C_{\text{corr}}$  and  $B_{\text{rec}}$  give correct centroids and relative total counts. Clearly this algorithm under experimental conditions will not give such accurate results because it is based on the assumptions given above and because of random variations in  $A$  and  $C$ . Work is progressing to study this.

It can be seen that column  $m$  of the  $A$  matrix is the profile of the peak that would be measured if an ion beam was incident above the  $m$ th detector. Therefore matrix  $A$  can be constructed by placing a beam of fixed intensity above each detector in turn, for a fixed time, and entering the measured peak profile in the corresponding column of  $A$  with the peak centre on the diagonal. It can be seen that information on

a)

DRC for detector number	Response to signal on detector number:										Incident spectrum	Measured spectrum
	0	1	2	3	4	5	6	7	8	9		
	0	1	.8	.4	.1	0	0	0	0	0		
1	.7	1	.8	.4	.03	0	0	0	0	0	0	.06
2	.1	.8	.5	.7	.3	.01	0	0	0	0	0	.66
3	0	.16	.7	0.9	.8	.4	.09	.02	0	0	0	4.18
4	0	0	.2	.83	1.3	.7	.4	.25	0	0	2	7.6
5	0	0	0	.2	.35	.8	.4	.15	.1	0	6	6.3
6	0	0	0	0	.2	.8	0.9	.2	.1	0	2	7
7	0	0	0	0	0	.3	.7	0.5	.6	.1	0	3.2
8	0	0	0	0	0	0	.1	0.5	1	.6	0	.2
9	0	0	0	0	0	0	.05	.4	.8	1	0	.1

A                          .                          B                          =                          C

$$\begin{bmatrix}
 1 & .7 & .35 & 0.1 & 0 & 0 & 0 & 0 & 0 & 0 & 0 \\
 0.7 & 1 & .7 & .35 & 0.1 & 0 & 0 & 0 & 0 & 0 & 0 \\
 0.35 & .7 & 1 & .7 & .35 & 0.1 & 0 & 0 & 0 & 0 & 0 \\
 0.1 & 0.35 & .7 & 1 & .7 & .35 & .1 & 0 & 0 & 0 & 0 \\
 0 & 0.1 & 0.35 & .7 & 1 & .7 & .35 & 0.1 & 0 & 0 & 0 \\
 0 & 0 & 0.1 & 0.35 & 0.7 & 1 & 0.7 & 0.35 & 0.1 & 0 & 0 \\
 0 & 0 & 0 & 0.1 & .35 & .7 & 1 & .7 & .35 & 0.1 & 0 \\
 0 & 0 & 0 & 0 & 0.1 & 0.35 & 0.7 & 1 & .7 & .35 & 0 \\
 0 & 0 & 0 & 0 & 0 & 0.1 & 0.35 & 0.7 & 1 & .7 & 0 \\
 0 & 0 & 0 & 0 & 0 & 0 & 0.1 & 0.35 & .7 & 1 & .7
 \end{bmatrix}$$

S

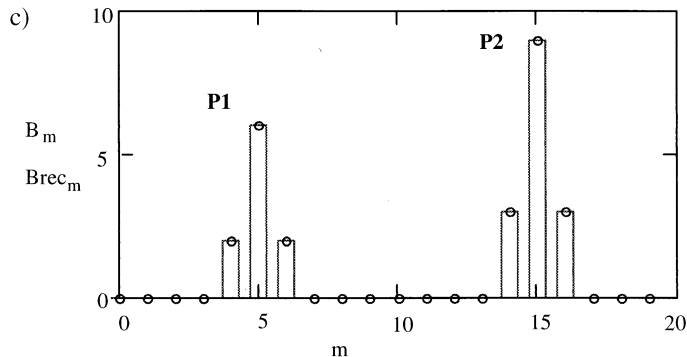
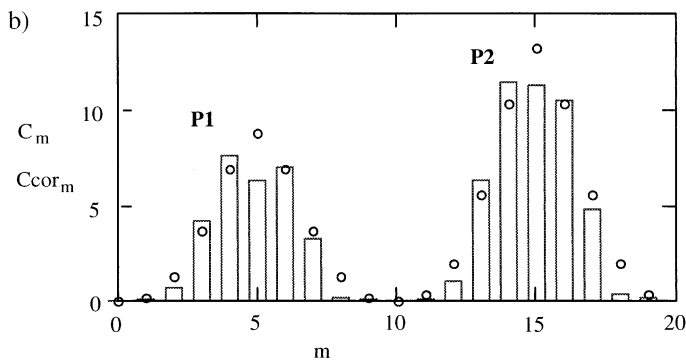


Fig. 4. (a) A  $10 \times 10$  section of the  $20 \times 20$  matrices used in the present calculations. (b) The spectrum measured (histogram) and corrected for nonuniformity (circles). Detectors are numbered 0–19. (c) The incident spectrum (histogram) and the recovered spectrum (circles).

Table 2

The centre of mass and total counts of two peaks in vectors  $B$  (the input spectrum),  $C$  (the measured spectrum),  $C_{\text{corr}}$  (the measured spectrum corrected for nonuniformity), and  $B_{\text{rec}}$  (the recovered incident spectrum)

Vector	$B$		$C$		$C_{\text{corr}}$		$B_{\text{rec}}$	
	P1	P2	P1	P2	P1	P2	P1	P2
Peak								
CofM	5	15	4.87	14.88	5	15	5	15
Total counts	10	15	29.3	45.75	33	49.5	10	15

nonuniformity of the MCP is contained in the rows of  $A$  and the columns contain information on the non-uniformity of the array.

The algorithm outlined above can be applied equally well to a 2D array of pixels. For computational purposes the pixels may be considered to be rearranged (in any order) into a column. The detector response curves for each pixel will not generally have the simple form as that for the 1D array but may be measured experimentally and combined to give the detector response matrix ( $A$ ). A measured spectrum ( $C$ ) is the column vector found by arranging the pixel outputs in the order given above and the incident image may be computed from  $A^{-1}C$  as a column vector. The 2D image may then be recovered by reassembling the elements of the recovered column vector.

### 3. Conclusions

An algorithm is presented that does not appear to have been used previously in the correction of non-uniformity. Assumptions have been made that the incident spectrum can be represented by a histogram and the detector response curves are measured as in Sec. 2.1.1 above. Work is progressing to understand the limitations introduced by these assumptions and to develop the algorithm for real applications including two dimensional array correction.

### References

- [1] D.P. Langstaff, M.W. Lawton, T.M. McGinnity, D.M. Forbes, K. Birkinshaw, *Meas. Sci. Technol.* 5 (1994) 389.
- [2] L.J. Richter, W. Ho, *Rev. Sci. Instrum.* 57 (1986) 1469.
- [3] K. Smith, *Exp. Meth. Phys. Sci.* 29A (1995) 253.
- [4] K. Birkinshaw, *Int. Revs. Phys. Chem.* 15 (1996) 13.
- [5] D.J. Narayan, D.P. Langstaff, M.P. Sinha, K. Birkinshaw, *Int. J. Mass Spectrom. Ion Processes* 176 (1998) 161.
- [6] M.P. Sinha, D.P. Langstaff, D.J. Narayan, K. Birkinshaw, *Int. J. Mass Spectrom. Ion Processes* 176 (1998) 99.
- [7] K. Birkinshaw, D.P. Langstaff, *Int. J. Mass Spectrom. Ion Processes* 136 (1994) 71.
- [8] D.J. Narayan, D.P. Langstaff, K. Birkinshaw, *Int. J. Mass Spectrom. Ion Processes* 149/150 (1995) 439.